Renewable Energy 57 (2013) 216–222

Contents lists available at SciVerse ScienceDirect

Renewable Energy

journal homepage: www.elsevier.com/locate/renene

Construction and preliminary test of a low-temperature regenerative Organic Rankine Cycle (ORC) using R123

Maoqing Li [a], Jiangfeng Wang [a], Weifeng He [a], Lin Gao [b], Bo Wang [a], Shaolin Ma [a,c], Yiping Dai [a,*]

[a] *Institute of Turbomachinery, Xi'an Jiaotong University, Xi'an, Shaanxi 710049, China*
[b] *Xi'an Thermal Power Research Institute Co., Ltd, Xi'an 710032, China*
[c] *Dongfang Steam Turbine Works, Deyang 618201, China*

ARTICLE INFO

Article history:
Received 8 June 2012
Accepted 28 January 2013
Available online 27 February 2013

Keywords:
Geothermal
Regenerative
Organic Rankine Cycle
Leakage issue
Efficiency

ABSTRACT

Higher efficiencies and optimal utilization of geothermal energy require a careful analysis of Organic Rankine Cycle (ORC) which is suitable for converting electric power from low-temperature heat sources. The objective of this study is to experimentally analyze the effect of varying working fluid mass flow rate and the regenerator on the efficiency of the regenerative ORC operating on R123. As R123 presents a low boiling point temperature (27.82 °C), a technology was invented to address the leakage issue when transferring R123 between the inside and outside of the regenerative ORC system. A specially manufactured throttle valve was adopted in the bypass subsystem to protect the turbine during the starting and closing processes and a novel phenomenon was discovered during the test. A preliminary test of the system was conducted with a geothermal source temperature of 130 °C. The experimental results show that the power output is 6 kW and the regenerative ORC efficiency is 7.98%, which is higher than that of the basic ORC by 1.83%.

1. Introduction

Rapid increase of the energy consumption has led to environmental pollution and energy shortage. Renewable energy sources are alternatives to the depleting conventional energy sources. Geothermal energy, a traditional renewable energy source, can be utilized in several ways. Most commonly, it is used in electric power generation [1]. Dipippo [2–8] investigated several types of geothermal power plants and he pointed out that the binary-type energy conversion systems with thermal efficiencies in the range of 8%–12% were typically used to exploit low-temperature geothermal resources. Among the different technical variations of binary systems, the Organic Rankine Cycle (ORC) system is the most widely used. ORC systems with organic mediums, which boil at a lower temperature than that of the water, have several advantages in utilizing low-grade energy [9,10]. Higher thermal efficiency and optimal utilization of the heat source require a careful selection of the working fluid. However, some characteristics other than system thermal efficiency should be considered when selecting an organic fluid to be used in ORC, such as toxicity, flammability, global warming potential (GWP), and ozone depletion potential (ODP) [11]. Yari et al. [12] investigated different geothermal concepts and several dry fluids for ORC by first and second law analysis. They indicated that the ORC with an internal heat exchanger and using R123 as the working fluid had the highest efficiency. Mago et al. [13] presented a second law analysis for the use of ORC to convert low-grade heat to power. They found that R123 showed the best efficiencies for heat source temperatures between 380 and 430 K. Tzu-Chen [14] investigated the working fluids Benzene (C_6H_6), Toluene (C_7H_8), p-xylene (C_8H_{10}), R113 and R123. He reported that R123 had a better performance in recovering a low-temperature waste heat. Huijuan et al. [15] presented a review of the ORC and supercritical Rankine cycle with 35 working fluids. They indicated that the critical temperature of R123 was above 400 K and this made R123 more likely to be used in ORC for utilizing low-temperature heat sources. Roy et al. [16] examined the output power and system efficiencies of an ORC using R12, R123 and R134a for waste heat recovery. It was discovered that R123 produced the maximum efficiencies and turbine power output with minimum irreversibility. As mentioned above, R123 is highly competitive working fluid when ORC is used to generate electricity from low-grade heat sources with temperature between 380 and 430 K. Moreover, R123 is nonflammable and noncorrosive [17].

In order to improve the performance of ORCs, several researchers investigated the regenerative ORC. Mago et al. [18] found that the regenerative ORC produced higher efficiency than the basic ORC after

* Corresponding author. Tel./fax: +86 (0)29 82668704.
E-mail addresses: ypdai@mail.xjtu.edu.cn, daiyiping.turbine@gmail.com (Y. Dai).

0960-1481/$ – see front matter © 2013 Elsevier Ltd. All rights reserved.
http://dx.doi.org/10.1016/j.renene.2013.01.042

Nomenclature

H	enthalpy, kJ kg^{-1}
P	pressure, Pa
Q	heat rate, kW
W	power, kW
Greek letters	
η	efficiency
ε	machine efficiency
Subscripts	
1–13	state points
g	generator
p	pump
t	turbine
s	isentropic process
e	net output

comparing the two systems by using a combined first and second law analysis. Desai et al. [19] analyzed 16 different working fluids for the basic as well as the regenerative ORC. The results indicated that by adopting a regenerator the thermal efficiency of the ORC would be improved by approximately 16.5%. Rong JX et al. [20] proposed an ORC system with a vapor injector as the regenerator. They indicated that the cycle could perform better than the basic ORC when the injector inlet vapor pressure was in certain regions.

Besides the numerical analysis, much research has been carried out to assess experimentally the ORC technology for power generation. For instance, Yanagisawa et al. [21] carried out an experimental study on an oil-free scroll-type air expander. It was observed that the maximal achieved volumetric and isentropic effectiveness were 76% and 60%, respectively. Mathias et al. [22] presented an experimental testing of a scroll expander producing 2.96 kW power from low-grade energy and the isentropic efficiency of the expander was 83%. Lemort et al. [23,24] conducted an experimental study on the prototype of an open-drive, oil-free scroll expander integrated into an ORC working with refrigerant R123. They showed that the maximum delivered shaft power and the maximum achieved overall isentropic effectiveness were 1.82 kW and 68%, respectively. Riffat et al. [25,26] designed and tested a 1.34 kW ORC for a CHP system assisted by fuel gas, and they discovered that the electrical efficiency and the overall efficiency were about 16% and 59%, respectively. Wang et al. [27] designed, constructed, and tested a prototype low-temperature solar ORC system with a rolling-piston expander. They discovered that when the output power was 1.73 kW the overall power generation efficiency was estimated at 4.2% or 3.2% for evacuated or flat plate collectors, respectively. Pei et al. [28] constructed a new kW-scale ORC system on the use of R123, the expander in the system was a specially designed and manufactured axial-radial-flow turbine. It was found that a turbine isentropic efficiency of 65% and an ORC efficiency of 6.8% could be obtained and the shaft power was 3.75 KW.

A review of the previous literature reveals that seldom information can be found on experimental research of the regenerative ORC, especially using the axial flow turbine. In this paper, the construction of a 10 kW scale regenerative ORC system and a preliminary test are proposed. A turbine-generator set was used to generate electricity, which was bypassed by a throttle valve during the starting and closing processes. The effects of the regenerator and the varying mass flow rate on the performance of the system were analyzed under a constant geothermal source temperature of 130 °C. Several problems solving techniques are presented, such as the avoidance of leakage of the R123. The system efficiency and electricity power were also evaluated.

2. Fundamental and structure

Fig. 1 shows the design chart of the low-temperature geothermal regenerative ORC system. The system consists of six subsystems: R123, bypass, geothermal water, lubricant oil, cooling water and working fluid replacement subsystems. The R123 subsystem is represented by solid lines while other subsystems are represented by dashed lines. The R123 subsystem consists of an evaporator, a pump, a turbine-generator set, a condenser and a regenerator. A cooling tower was used to keep the temperature of the cooling water equal to the outdoor temperature. In the regenerative Rankine cycle system, the working fluid (R123) is preheated with the energy of the turbine exhaust in a regenerator from state 1 to state 2, heated in an evaporator to state 3, expanded in a turbine to state 4, precooled in the regenerator to state 5, cooled down with the cooling water in a condenser to state 6 and compressed in a pump back to state 1. A liquid tank installed before the pump was used to ensure the normal operation of the pump. Like the conventional steam Rankine cycle, “pinch point” also exists in the heat exchangers, such as condenser and evaporator [29]. The effect of “pinch point” on the performance of the ORC system will be evaluated in the future.

The key thermodynamic state points are marked with circles around the numbers. The thermodynamic analysis is evaluated by the following equations given in Refs. [8,29]. High pressure R123 liquid from the pump is heated in the evaporator. The process involves preheating, evaporating and superheating as usual, while in the regenerative ORC system, the working fluid is preheated in the regenerator.

The heat absorption in the regenerator and the evaporator are

$$Q_1 = H_2 - H_1 \tag{1}$$

$$Q_2 = H_3 - H_2 \tag{2}$$

where Q_1, Q_2, H_1, H_2 and H_3 are the heat absorption in the regenerator, the heat absorption in the evaporator, the pump outlet enthalpy, the evaporator inlet enthalpy and the evaporator outlet enthalpy, respectively.

The expansion process in the turbine is usually not isentropic and the isentropic efficiency of the turbine is

$$\eta_t = \frac{H_3 - H_4}{H_3 - H_{4s}} \tag{3}$$

where η_t, H_4, and H_{4s} are the isentropic efficiency, the enthalpy of turbine outlet and the enthalpy of the turbine outlet through the ideal isentropic process, respectively, and H_{4s} can be calculated by the turbine inlet entropy and outlet pressure. The generated power depends on the real inlet and the outlet enthalpies is

$$W_t = H_3 - H_4 \tag{4}$$

The turbine exhaust is precooled in the regenerator and then condensed and supercooled in the condenser. The transferred heat from R123 to the cooling water in the condenser is

$$Q_4 = H_5 - H_6 \tag{5}$$

where Q_4, H_5 and H_6 are the heat transferred from R123 to the cooling water, the enthalpy of the inlet of the condenser and the enthalpy of the outlet of the condenser, respectively.

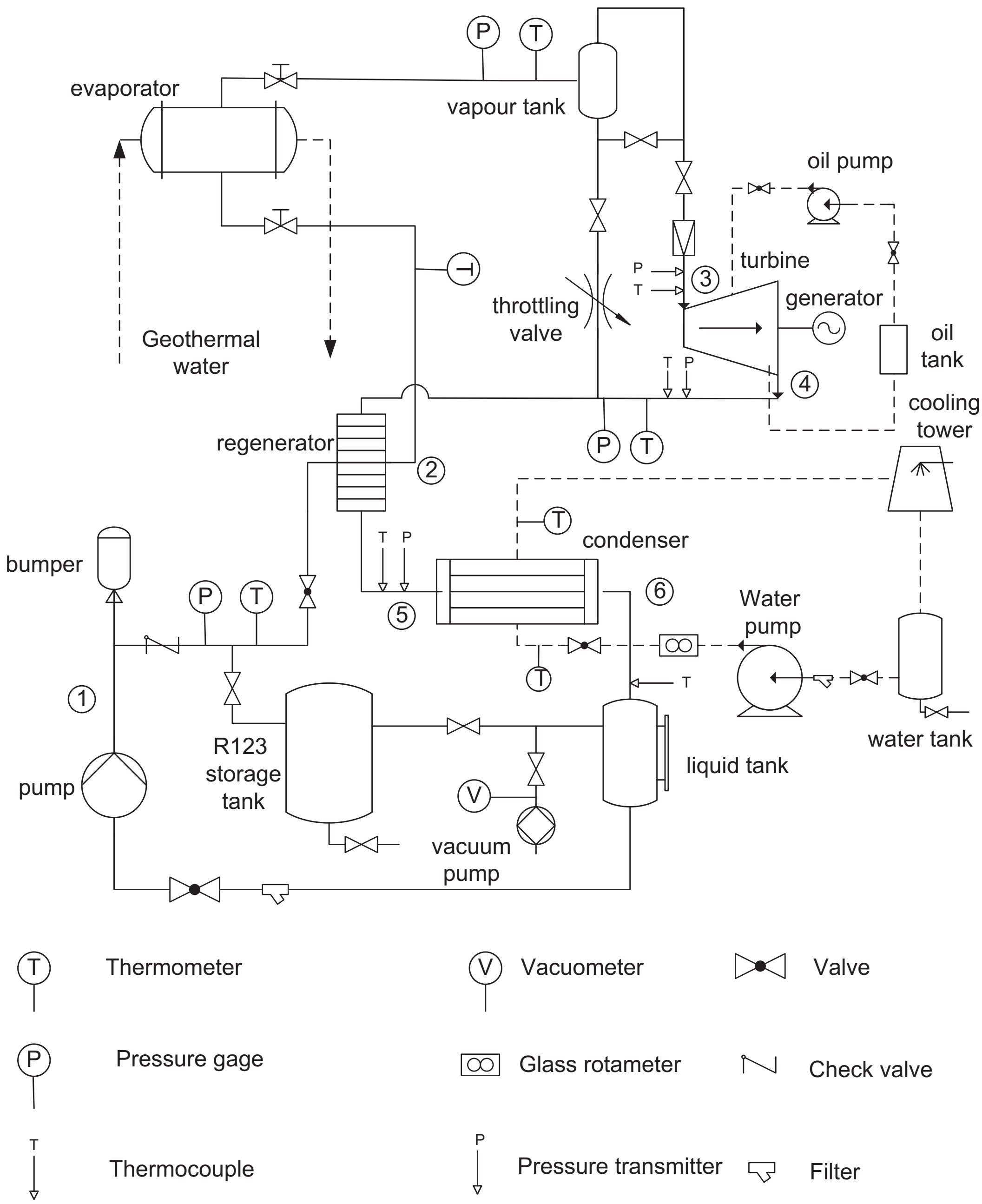

Fig. 1. Design chart of the RORC system.

In the pump, R123 is pumped to the set pressure and then enters into the regenerator. The power consumed by the pump is

$$W_p = H_1 - H_6 \tag{6}$$

The net shaft power of the turbine and the thermal efficiency of the system are calculated as follows:

$$W = W_t - W_p \tag{7}$$

$$\eta = \frac{W}{Q_2} = \frac{W_t - W_p}{Q_2} = \frac{(H_3 - H_4) - (H_1 - H_6)}{H_3 - H_2} \tag{8}$$

The output electric power is

$$W_e = W_t{}^*\varepsilon_g - W_p \tag{9}$$

where ε_g is the generator efficiency and the power consumption of the pump is generally negligible compared with the energy input in the refrigerant cycle [25].

3. Experimental investigation

The pump adopted in the system was a hydraulic diaphragm type pump. The piston transmitted the power to the fluid by the intermediary of a flexible membrane between the fluid and the piston, which allowed the use of abrasive or corrosive liquids. The choice of this pump was for two purposes: one was resisting the R123 working fluid, which was very corrosive to synthetic materials; the other was avoiding cavitation, which was common when using a centrifugal pump. A bumper was installed at the position outlet of the pump to absorb the shock and smooth the fluid pressure into heat exchangers. The flow rate could be adjusted by a manual graduated gearbox at the broadside of the pump.

An electric heater using conduction oil to heat R123 was used as the geothermal energy source for convenience and its heating power (HP) and heating temperature (HT) could be both decided. During the test, the temperature of the geothermal energy source was 130 °C which was the HT of the electric heater. When the R123 liquid absorbed heat and evaporated in the electric heater, the oil temperature decreased. Once the oil temperature dropped below the HT, the electricity heat started to heat the conduction oil back to HT. And if the oil temperature exceeded HT, the electric heater would stop working. This process was carried out automatically by the electric heater after setting the HT manually. If the oil temperature couldn't reach back to HT due to a large R123 mass flow rate, the HP of the electricity must be increased manually.

Plate heat exchangers were adopted as both the regenerator and the condenser. The regenerator has 60 plates and the total heat exchange area is 5.51 m^2, while the condenser has 120 plates and the total heat exchange area is 11.21 m^2.

R123 is expensive, low toxicity and leaks especially easily when transferring R123 between the inside and outside of the regenerative ORC system due to its low boiling point. Therefore, it is difficult to inject R123 into the R123 subsystem before the test and retrieve R123 from the R123 subsystem after the test, respectively. Working fluid replacement system (WFRS) as shown in Fig. 2(a), which contains a storage tank, three valves and several pipes, is presented to deal with this issue. Before the test, R123 should be injected into the R123 subsystem from the storage tank. A vacuum pump was adopted to extract air from the R123 subsystem, with valve 2 open and the valves 1 and 3 closed. After applying vacuum supply to the R123 subsystem, R123 could flow into the system due to the pressure difference between WFRS and the R123 subsystem,

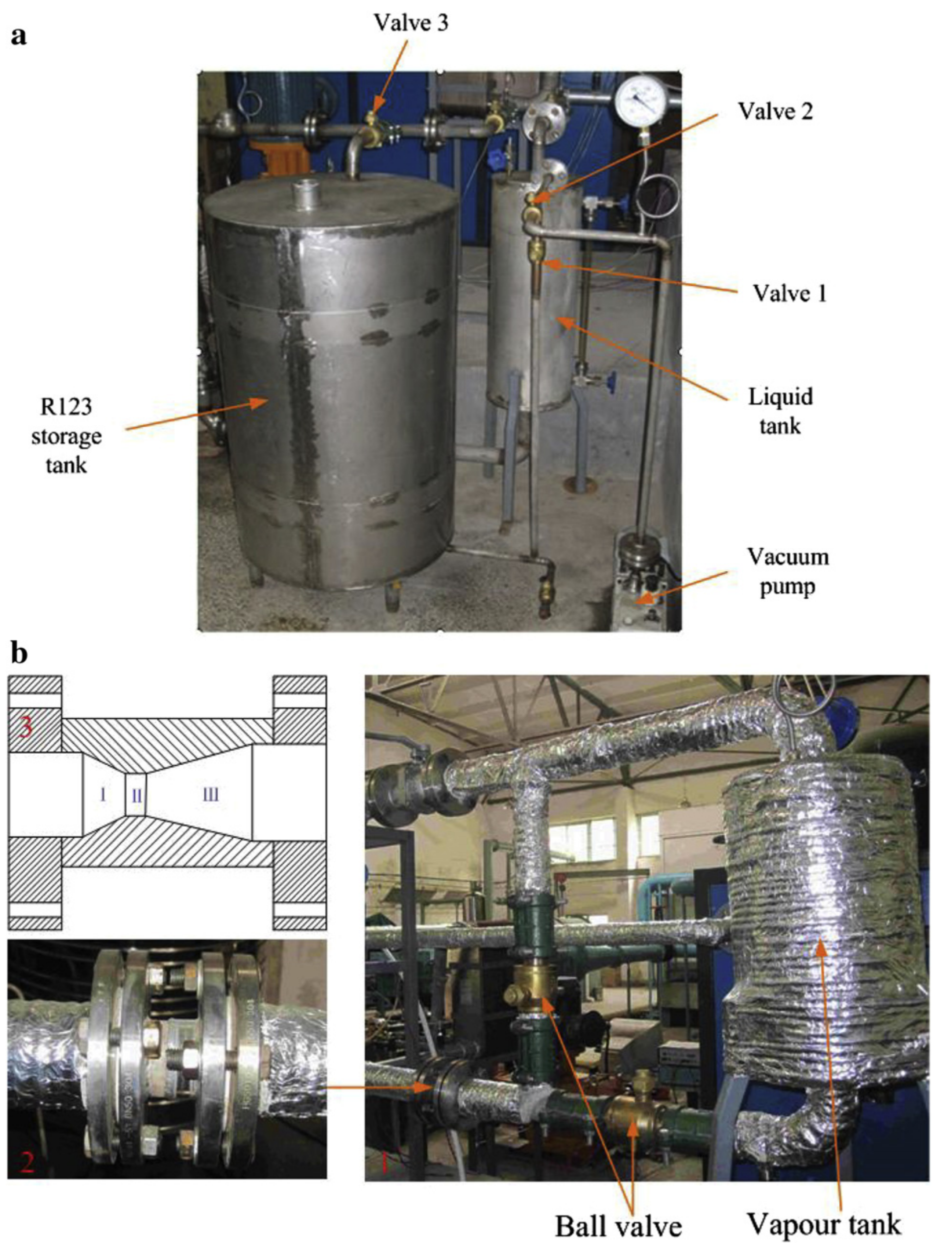

Fig. 2. Experimental layout of the system (a) Working fluid replacement system; (b) The bypass circuit and the throttling valve.

with valves 2 and 3 closed and the valve 1 open. The quantity of R123 that flowed into the R123 subsystem could be obtained by observing the fluid level in the liquid tank. When the liquid level reached to the set value, the three valves were all closed. After the test, the working fluid could be pumped back into the storage tank from the R123 subsystem while keeping the pump working, with valve 3 open and the other two valves closed. Using WFRS, the injection and retrieval of R123 could be convenient and effective.

A single stage axial flow turbine was adopted in this test. A generator was connected to the turbine with a coupler. Using an asynchronous machine is a convenient way to impose the rotational speed of the turbine.

The bypass subsystem, where a throttle valve was installed, was used in this system to bypass the turbine during the starting and closing process. In these two processes, R123 is usually two phase condition at the evaporator outlet and that is harmful to the blades if the two phase fluid passes through the turbine. Therefore, a throttle valve was designed and fabricated (shown in Fig. 2(b1)) to deal with this issue. As R123 has a lower local sonic speed compared to the water caused by higher molecular weight, the throttle valve was designed specially according to its thermo-physical properties.

The throttle valve was assembled in the regenerative ORC system using flanges welded at both of its ends as shown in Fig. 2(b2). The design pressure at the throttling valve outlet was a little higher than the atmosphere pressure. The throttle valve contains three sections as shown in Fig. 2(b3): constricted section (I), throat (II), and diffuser (III). The diameter of the throat section is 9.57 mm. The throat length was designed as 4 mm for the convenience of manufacture and this had no effect on the expansion of R123. The outlet diameter and the length of the diffuser are 16.81 mm and 13.44 mm, respectively.

An orifice plate flow meter coupled with a pressure difference transmitter was used as the flow meter with measurement accuracy ±0.83% and a measuring range of 1600 L/h. A glass tube float flow meter was used to measure the cooling water flow rate through the condenser. Copper-constantan thermocouples were used to measure the temperature, with an accuracy of ±0.1 °C. Pressure transmitters with an accuracy of ±235.98 Pa, were used in the experiment to measure the pressure. Rotation speed was measured by the turbine dynamic speed measurement device, with an accuracy of ±1‰. An electricity counter with an accuracy of ±3% was used to measure the amount of electrical energy produced by the asynchronous machine. The measurement data were recorded and stored automatically by the computer. The calculated parameters included shaft power and the system efficiency.

4. Experiment results

During the experimental test, the R123 mass flow rate increased step by step while the evaporation temperature was unchanged.

Fig. 3 shows the turbine rotation speed and R123 mass flow rate varying with time. The mass flow rate was measured by the flow meter and was equal to that through the pump. At 19:52 PM, the turbine rotation speed increased suddenly with the sudden surge in the mass flow rate, while at 20:20 PM, the rotation speed of the turbine decreased suddenly with the sudden decrease in the mass flow rate. From 19:52 PM to 20:20 PM, turbine rotation speed increased to a maximum value of 3014 rpm and the variation tendency was very similar to the mass flow.

The pressure and temperature at the turbine inlet varying with time is shown in Fig. 4. As the HT of the electric heater was set at 130 °C, the turbine inlet temperature was about 120 °C due to the terminal temperature difference in the evaporator. The turbine inlet pressure increased step by step with several peaks. The curve variation trend of the turbine inlet pressure was similar to that of the mass flow rate.

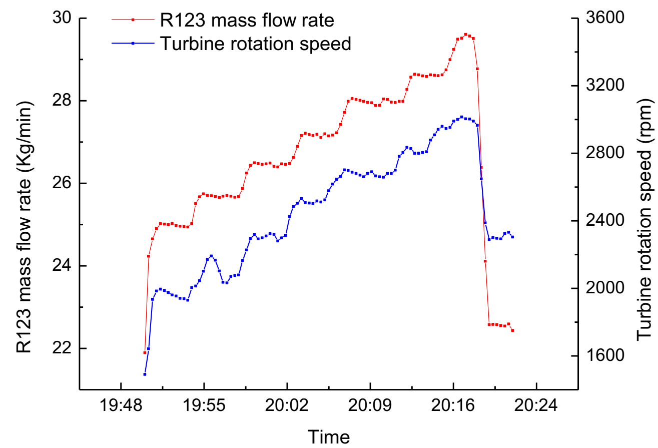

Fig. 3. Turbine rotation speed and R123 mass flow rate vs. time.

The turbine outlet pressure, turbine outlet temperature and pump outlet temperature over time is shown in Fig. 5. The turbine outlet temperature decreased slightly from 19:52 PM to 20:20 PM. The reason was that with increasing turbine rotation speed from 19:52 PM to 20:20 PM shown in Fig. 3, the isentropic efficiency of the turbine increased and this led to a decrease in the turbine outlet temperature. The temperature of the pump outlet, which was equal to the condenser outlet temperature due to the fact that heat loss between the condenser and the pump was very small, increased slightly from 19:52 PM to 20:20 PM. During this test, the cooling water mass flow rate, the cooling water temperature and the condenser heat exchange area were all unchanged. The condensing temperature was decided by the R123 mass flow rate and the turbine outlet temperature. Therefore, the condensing temperature increased with increasing R123 mass flow rate, though the turbine outlet temperature decreased. Turbine outlet pressure is decided by the condensing temperature, and as analyzed above the condensing temperature is mainly decided by the R123 mass flow rate. So, the turbine outlet pressure is decided by the R123 mass flow rate. It is obvious that the variance of the turbine outlet pressure shown in Fig. 5 is similar to that of the R123 mass flow rate shown in Fig. 3. Figs. 3 and 5 reveal that the turbine outlet pressure increases and decreases with the increasing and decreasing R123 mass flow rate, respectively.

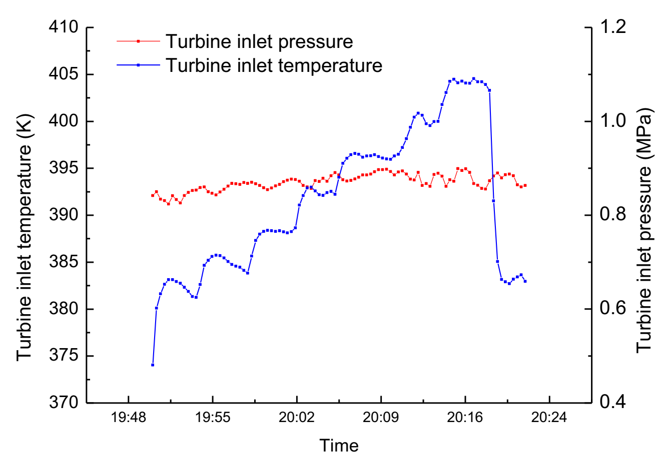

Fig. 4. Turbine inlet pressure and temperature vs. time.

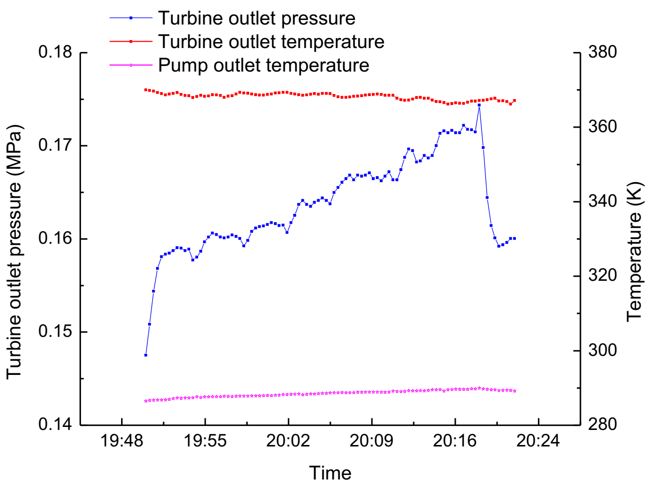

Fig. 5. Turbine outlet pressure and temperature and pump outlet temperature vs. time.

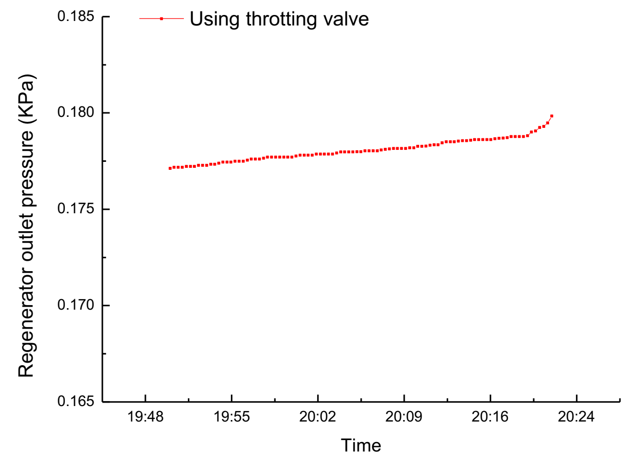

Fig. 7. Regenerator outlet pressure vs. time.

The temperature and the pressure at the regenerator outlet varying with time is shown in Fig. 6. Compared with the turbine outlet pressure, the regenerator outlet pressure was lower. The maximum of the pressure difference between the regenerator outlet and the turbine outlet was 25.5 kPa. The regenerator which is the plate heat exchanger is mainly responsible for this phenomenon. The temperature and pressure data in Fig. 6 also showed that R123 at the regenerator outlet was in the two phase region. As a preliminary test, a regenerator with a large margin area was selected in the construction process and this was responsible for the situation. A novel phenomenon caused by the two phase flow at the regenerator outlet was discovered and which is shown below.

When the throttle valve was opened quickly during the closing process of the system, the liquid level of the liquid tank rose up rapidly. This puts the liquid tank in danger, especially to the transparent liquid level indicator installed in the liquid tank. To obtain a general understanding of the relationship between the throttle valve and the liquid level, the regenerator outlet pressure when using the throttle valve was examined. Fig. 7 shows the pressure of the regenerator outlet varying with time as R123 passes through the throttle valve. When R123 expanded in the throttle valve, the regenerator outlet pressure was higher than that when R123 expanded in the turbine which was shown in Fig. 5. The reason could be that the throttle valve is self-designed and manufactured and the expansion ratio is not enough due to design error and foozle manufacture, therefore, the throttle valve outlet pressure is higher than that of the turbine outlet.

The two phase flow (shown in Fig. 6) from the regenerator was cooled down to pure liquid immediately in the condenser. As an estimate, at least one half of the condenser was full of pure liquid. The pure liquid stayed in the condenser as a result of the pressure balance between the regenerator outlet and the liquid tank until when the throttle valve was opened quickly. This is because the increased regenerator outlet pressure (shown in Fig. 7) made the liquid in the condenser flow into the liquid tank and led to an abruptly rising in the liquid level. To avoid this phenomenon, the throttle valve must be opened slowly while observing the fluid level of the liquid tank during the closing process of the system.

The performance of the ORC systems could be evaluated by the heat recovery, especially when ORC is adopted to utilize a low-temperature heat source. To obtain the relationship between the regenerator and the performance of the ORC, Regenerator Efficiency (RE) is proposed. RE is defined as the rate of specific heat absorption in the regenerator and the total specific heat absorption in the ORC system. The RE varying with time is shown in Fig. 8. As shown in Fig. 8, RE decreased with several peaks from 19:52 PM to 20:20 PM. As the heat transfer area of the regenerator is constant, the heat transfer from the vapor of the turbine outlet to the liquid of the pump outlet is determined by the mean temperature difference

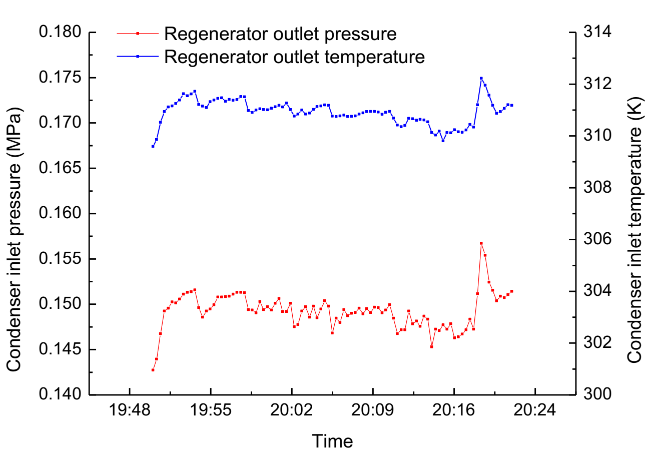

Fig. 6. Regenerator outlet pressure and outlet temperature vs. time.

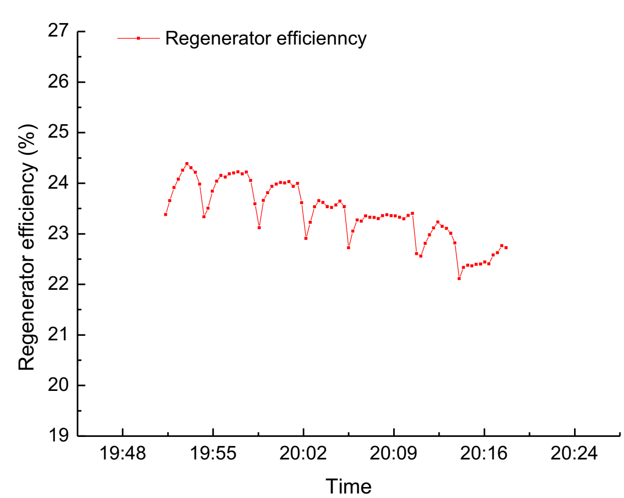

Fig. 8. Regenerator efficiency vs. time.

Table 1
Calculated thermodynamic properties of the working fluid in the regenerative ORC.

State point	Pressure (kPa)	Temperature (K)	Mass flow rate (kg/s)	Enthalpy (kJ/kg)	Entropy (kJ/(kg K)
1	640.9	287.33	0.403	214.37	1.0498
2	634.4	341.22	0.403	270.39	1.2284
3	626.9	392.6	0.403	459.12	1.7473
4	158.7	365.0	0.403	444.05	1.7773
5	151.4	311.62	0.403	239.0	1.1333
6	139.9	287.59	0.403	214.46	1.0513

Table 2
Analysis of the regenerative ORC system.

Item	Energy load (kW)	Efficiency (%)
Regenerator	22.58	29.69
Evaporator	76.06	\
Turbine	6.07	58.53
Condenser	9.89	\
Basic ORC system	\	6.15
Regenerative ORC system	\	7.98

in the regenerator. The temperature difference in the regenerator decreased varying with time, since the vapor temperature of the turbine outlet and the liquid temperature of the pump outlet decreased and increased, respectively, as shown in Fig. 5. This led to a decrease heat transfer in the regenerator and a decrease in RE due to the total specific heat absorption was nearly unchanged. In addition, the variation of the liquid temperature of the pump outlet and the vapor temperature of the turbine outlet is decided by the R123 mass flow rate as analyzed above. Therefore, the variation of RE obtained in this test revealed that the effect of the regenerator on the performance of the ORC system receded when the mass flow rate increased.

The specifications of the regenerative ORC thermodynamic properties on a relatively steady operating condition are listed in Table 1. The energy analysis of the regenerative ORC components, turbine efficiency and system efficiency are presented in Table 2. Table 2 shows that, the electric power generated by the system was 6.07 kW and the turbine efficiency was 58.53%. The efficiency of the basic ORC was also calculated which was lower than the regenerative ORC's by about 1.83%. The research discovered that the regenerator could effectively increase the heat recapture of ORC system when utilizing low-grade waste heat.

5. Conclusion

In this study, a low-temperature geothermal regenerative ORC system working with R123 is designed and built. A preliminary test of the experimental system is executed and several problems, such as R123 leakage issues when pouring it into the system, are solved. The effect of the increasing mass flow rate with unchanged geothermal source temperature on the system performance is evaluated. With increasing mass flow rate, the turbine inlet pressure and the turbine rotation speed both increase while the regenerator efficiency performs oppositely. The experimental data show that the maximum regenerator efficiency is 24.5%. The electric power generated by the system is 6.07 kW with a turbine efficiency of 58.53%. The efficiency of the regenerative ORC is 7.98%, higher than that of the basic ORC by about 1.83%.

As a preliminary test, the regenerative ORC is evaluated under just one geothermal condition in terms of thermal efficiency. In the future, the experimental system would be updated and evaluated by means of combined thermal efficiency and exergy efficiency under varying geothermal conditions.

Acknowledgment

The study presented in this paper is financially supported by National Key Technology R&D Program (No.2011BAA05B03) and the National Natural Science Foundation of China (Grant No. 51106117).

References

[1] Aljundi IH. Effect of dry hydrocarbons and critical point temperature on the efficiencies of organic rankine cycle. Renewable Energy 2011;36:1196–202.
[2] DiPippo R. Ideal thermal efficiency for geothermal binary plants. Geothermics 2007;36:276–85.
[3] Moya P, DiPippo R. Unit 5 bottoming binary plant at Miravalles geothermal field, Costa Rica: planning, design, performance and impact. Geothermics 2007;36:63–96.
[4] DiPippo R. Vacuum flash geothermal power plants: second law analysis and optimization. E. Amer Inst Chem; 1997.
[5] Dipippo R, Dipippo EA, Kestin J, Khalifa HE. Compound hybrid geothermal-fossil power-plants – thermodynamic analyses and site-specific applications. Journal of Engineering for Power-Trans Asme 1981;103:797–804.
[6] DiPippo R. Exergy analysis of combined electricity and direct-heat geothermal flash-steam plants. Geothermal Research Council Transactions 1987; 11:411–6.
[7] DiPippo R. Second law analysis of flash-binary and multilevel binary geothermal power plants. Transactions-Geothermal Resources Council 1994:505.
[8] DiPippo R. Second law assessment of binary plants generating power from low-temperature geothermal fluids. Geothermics 2004;33:565–86.
[9] Badr O, Probert SD, Ocallaghan PW. Selecting a working fluid for a Rankine-cycle engine. Applied Energy 1985;21:1–42.
[10] Dai YP, Wang JF, Gao L. Parametric optimization and comparative study of organic Rankine cycle (ORC) for low grade waste heat recovery. Energy Conversion and Management 2009;50:576–82.
[11] Saleh B, Wendland M. Screening of pure fluids as alternative refrigerants. International Journal of Refrigeration-Revue Internationale Du Froid 2006;29: 260–9.
[12] Yari M. Performance analysis of the different Organic Rankine Cycles (ORCs) using dry fluids. International Journal of Exergy 2009;6:323–42.
[13] Mago PJ, Chamra LM, Somayaji C. Performance analysis of different working fluids for use in organic Rankine cycles. Proceedings of the Institution of Mechanical Engineers Part A-Journal of Power and Energy 2007;221:255–64.
[14] Tzu-Chen H. Waste heat recovery of organic Rankine cycle using dry fluids. Energy Conversion and Management 2001;42.
[15] Huijuan C, Goswami DY, Stefanakos EK. A review of thermodynamic cycles and working fluids for the conversion of low-grade heat. Renewable and Sustainable Energy Reviews 2010;14.
[16] Roy JP, Mishra MK, Misra A. Performance analysis of an Organic Rankine Cycle with superheating under different heat source temperature conditions. Applied Energy 2011;88:2995–3004.
[17] Wang JF, Dai YP, Gao L, Ma SL. A new combined cooling, heating and power system driven by solar energy. Renewable Energy 2009;34:2780–8.
[18] Mago PJ, Chamra LM, Srinivasan K, Somayaji C. An examination of regenerative organic Rankine cycles using dry fluids. Applied Thermal Engineering 2008;28:998–1007.
[19] Desai NB, Bandyopadhyay S. Process integration of organic Rankine cycle. Energy 2009;34:1674–86.
[20] Rong-Ji X, Ya-Ling H. A vapor injector-based novel regenerative organic Rankine cycle. Applied Thermal Engineering 2011;31.
[21] Yanagisawa T, Fukuta M, Ogi Y, Hikichi T, Imeche. Performance of an oil-free scroll-type air expander. In: International conference on compressors and their systems. London, England: City Univ London; 2001. p. 167–74.
[22] Mathias JA, Johnston JR, Cao JM, Priedeman DK, Christensen RN. Experimental testing of gerotor and scroll expanders used in, and energetic and exergetic modeling of, an Organic Rankine Cycle. Journal of Energy Resources Technology-Asme 2009;131.
[23] Lemort V, Quoilin S, Cuevas C, Lebrun J. Testing and modeling a scroll expander integrated into an Organic Rankine Cycle. Applied Thermal Engineering 2009;29:3094–102.
[24] Quoilin S, Lemort V, Lebrun J. Experimental study and modeling of an Organic Rankine Cycle using scroll expander. Applied Energy 2010;87:1260–8.
[25] Riffat SB, Zhao X. A novel hybrid heat pipe solar collector/CHP system – part 1: system design and construction. Renewable Energy 2004;29:2217–33.
[26] Riffat SB, Zhao X. A novel hybrid heat-pipe solar collector/CHP system – part II: theoretical and experimental investigations. Renewable Energy 2004;29: 1965–90.
[27] Wang XD, Zhao L, Wang JL, Zhang WZ, Zhao XZ, Wu W. Performance evaluation of a low-temperature solar Rankine cycle system utilizing R245fa. Solar Energy 2010;84:353–64.
[28] Pei G, Li J, Li Y, Wang D, Ji J. Construction and dynamic test of a small-scale organic rankine cycle. Energy 2011;36:3215–23.
[29] DiPippo R. Geothermal power plants: principles, applications, case studies and environmental impact. Butterworth-Heinemann; 2012.